Supplementary Information

Functional group tuning of CAU-10(Al) for efficient C_2H_2 storage and C_2H_2/CO_2 separation

Eun Woo Lee[†a], Balkaran Singh Sran[†a], Ayoub Daouli[†c], Maftun Salimov [ab], Ji Woong Yoon[a], Kyung Ho Cho[ab], Donghui Jo[a], Guillaume Maurin*[c], Su-Kyung Lee*[ab], U-Hwang Lee*[ab]

a. Research Group for Nanocatalysts and Center for Convergent Chemical Process (CCP), Korea Research Institute of Chemical Technology (KRICT), Gajeong-Ro 141, Yuseong, Daejeon 34114, Republic of Korea.
b. Department of Advanced Materials and Chemical Engineering, University of Science and Technology (UST), Daejeon 34113, Republic of Korea
c. ICGM, University Montpellier, CNRS, ENSCM, Montpellier, France

E-mail: guillaume.maurin1@umontpellier.fr (G. Maurin), sukyung@krict.re.kr (S.-K. Lee), uhwang@krict.re.kr (U.-H. Lee)

† These authors contributed equally to this work.

IR Spectroscopy :

Vibration (type)*	Literature	CAU-10-H	CAU-10-OH	CAU-10-F	CAU-10-NO_2	CAU-10-NH_2	CAU-10-CH_3
$\nu_{s\,(}$ μ-$OH_{)}$	3600-3650	3616	3610	3621	3644	3610	3612
$\nu_s(CH)_{methyl}$	2930	-	-	-	-	-	2928
$\nu_s(CH)_{ring}$	3000-3100	3078	3080	3085	3080	3073	3082
$\nu_s(CH)_{out\ of\ plain\ bending}$	720	-	-	-	-	-	729
N-H wagging band	764	-	-	-	-	781	-
symmetric stretching NH_2	3448	-	-	-	-	Merged with OH peak	-
asymmetric stretching NH_2	3368	-	-	-	-	Merged with OH peak	-
ν_s(COO)	1550-1580	1554	1568	1578	1547	1563	1568
[ν_{as}(COO)]	1390-1450	1400	1415	1401	1400	1405	1401
C-O stretching	1120	1097	1129	1115	1097	1108	1114
[ν_s(CF)]	1240	-	-	1272	-	-	-
ν_{as}(NO)	1547	-	-	-	1547	-	-
ν_s(NO)	1340–1360	-	-	-	1350	-	-
$\nu_s\,(OH)_{water}$	3300-3500	3414	3419	3416	3410	3380	3390

Table S1. IR spectroscopy analysis of CAU-10-X

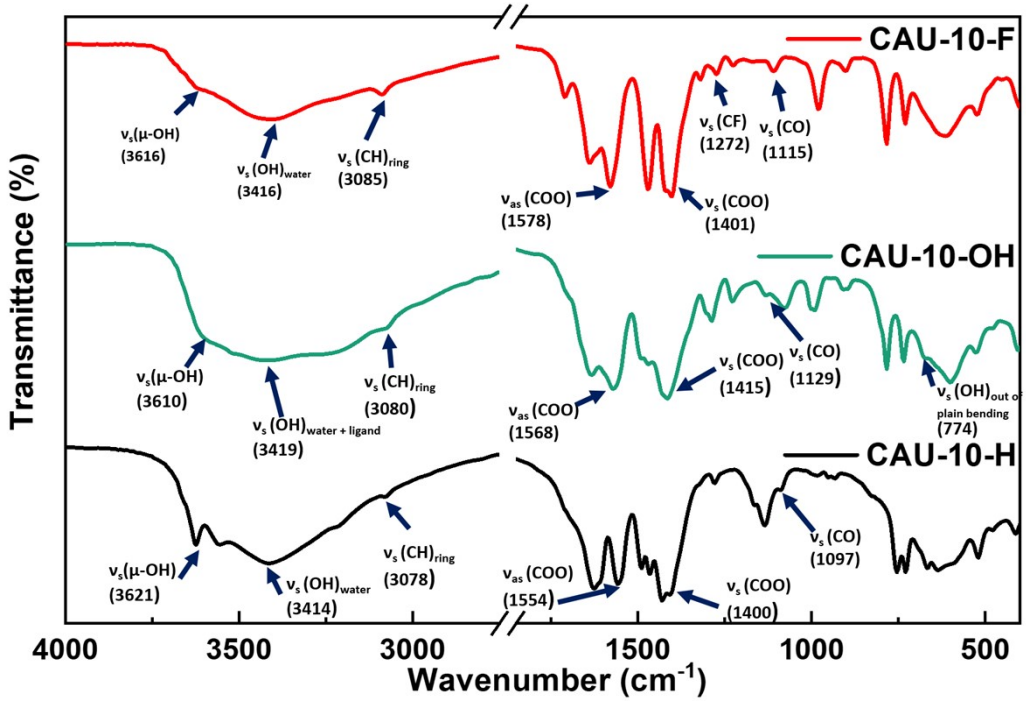

Fig. S1 FT-IR spectra of CAU-10-H (black), CAU-10-OH (green) and CAU-10-F (red).

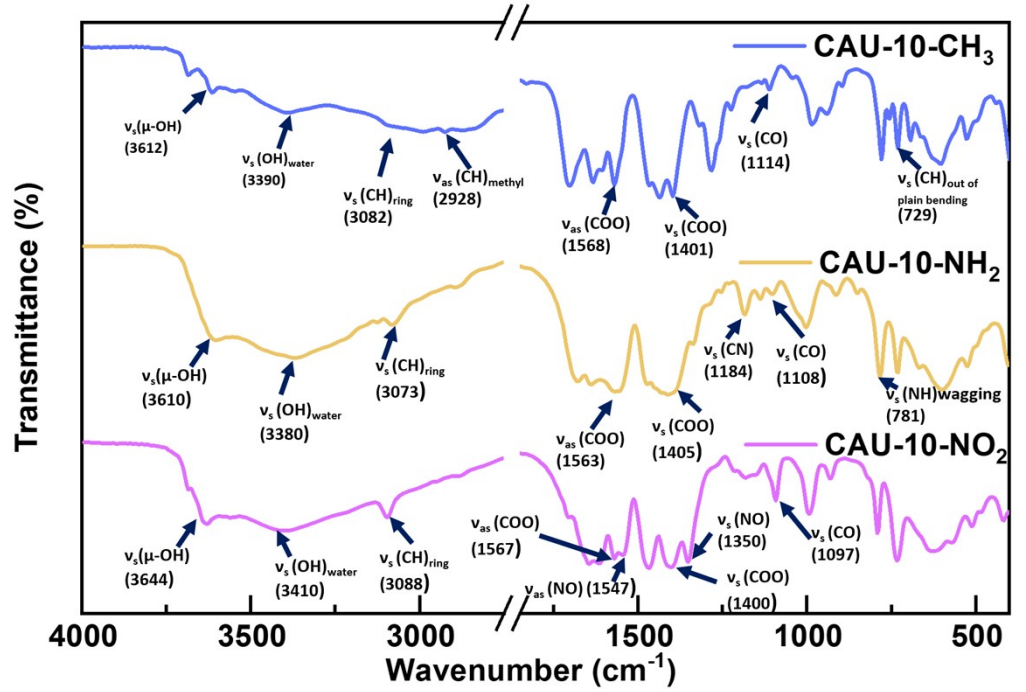

Fig. S2 FT-IR spectra of CAU-10-NO_2 (purple), CAU-10-NH_2 (yellow) and CAU-10-CH_3 (blue).

Thermogravimetric analysis (TGA):

Table S2. TGA analysis of CAU-10-X samples.

MOF	Water in the sample (%)	Theoretical Amount of Ligand (%)	Experimental Amount of Ligand *	Theoretical Amount of Residue (Al_2O_3) dehydrated (%)	Experimental Amount of Residue (Al_2O_3) (%)*
CAU-10-H	24.51	78.86	76.16	24.49	23.84
CAU-10-OH	20.4	80.37	75.2	22.74	24.8
CAU-10-F	18.4	80.54	77.26	22.54	22.74
CAU-10-NO_2	15.83	82.61	81.47	20.14	18.53
CAU-10-NH_2	14.32	80.28	79.12	22.84	20.88
CAU-10-CH_3	12.2	80.19	76.58	22.95	23.42

*after doing water weight percentage correction

The following formula was used to include water weight correction:

$$Wc = \frac{A \times W}{100} + A$$

Where Wc : % Weight of component for dehydrated sample

W : % Weight of water calculated from TGA curve

A : % Weight of component from calculated from TGA curve

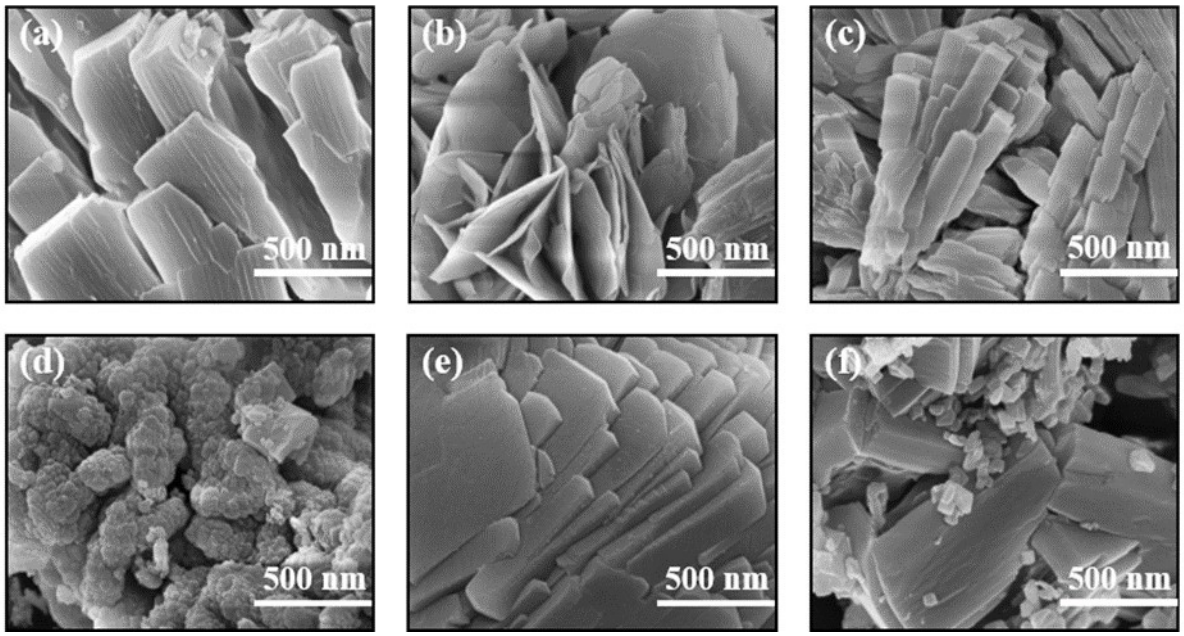

Fig. S3 Scanning electron microscope images of (a) CAU-10-H (b) CAU-10-OH (c) CAU-10-F (d) CAU-10-NO_2 (e) CAU-10-NH_2 (f) CAU-10-CH_3.

Table S3. Elemental analysis of CAU-10-X

Sample	Element [atom %]			
	C	H	O	N
CAU-10-H	46.8	31.6	21.7	N.D
CAU-10-OH	39.8	32.9	27.1	N.D
CAU-10-NO_2	40	25	30	5
CAU-10-NH_2	38.6	34.3	22.4	4.7
CAU-10-CH_3	45	36.7	18.6	N.D

N,D denotes non-detectable, and the detection limit of the sample is 0.1 wt%; CAU-10-F having fluorine is not indicated because EA is not possible

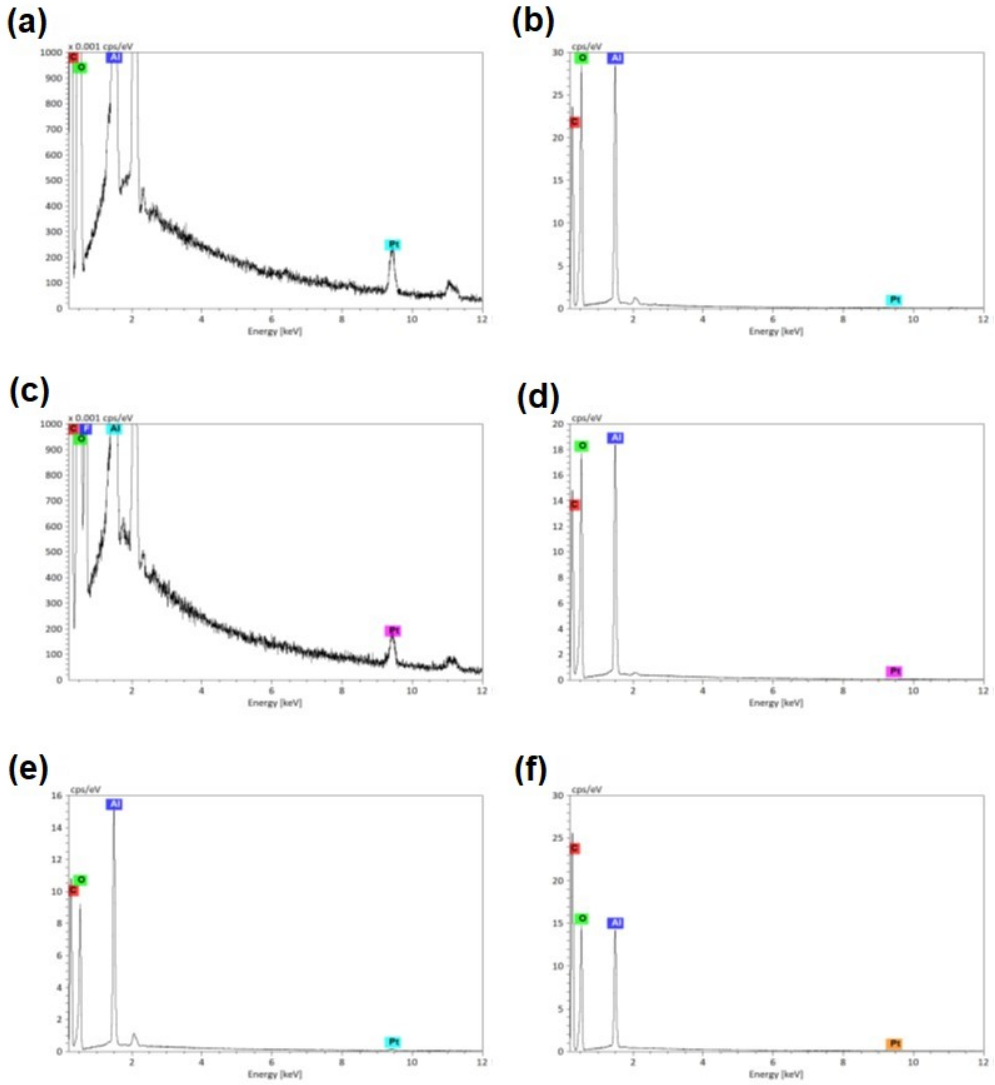

Fig. S4 X-ray energy dispersive spectroscopy analysis of (a) CAU-10-H (b) CAU-10-OH (c) CAU-10-F (d) CAU-10-NO_2 (e) CAU-10-NH_2 (f) CAU-10-CH_3.

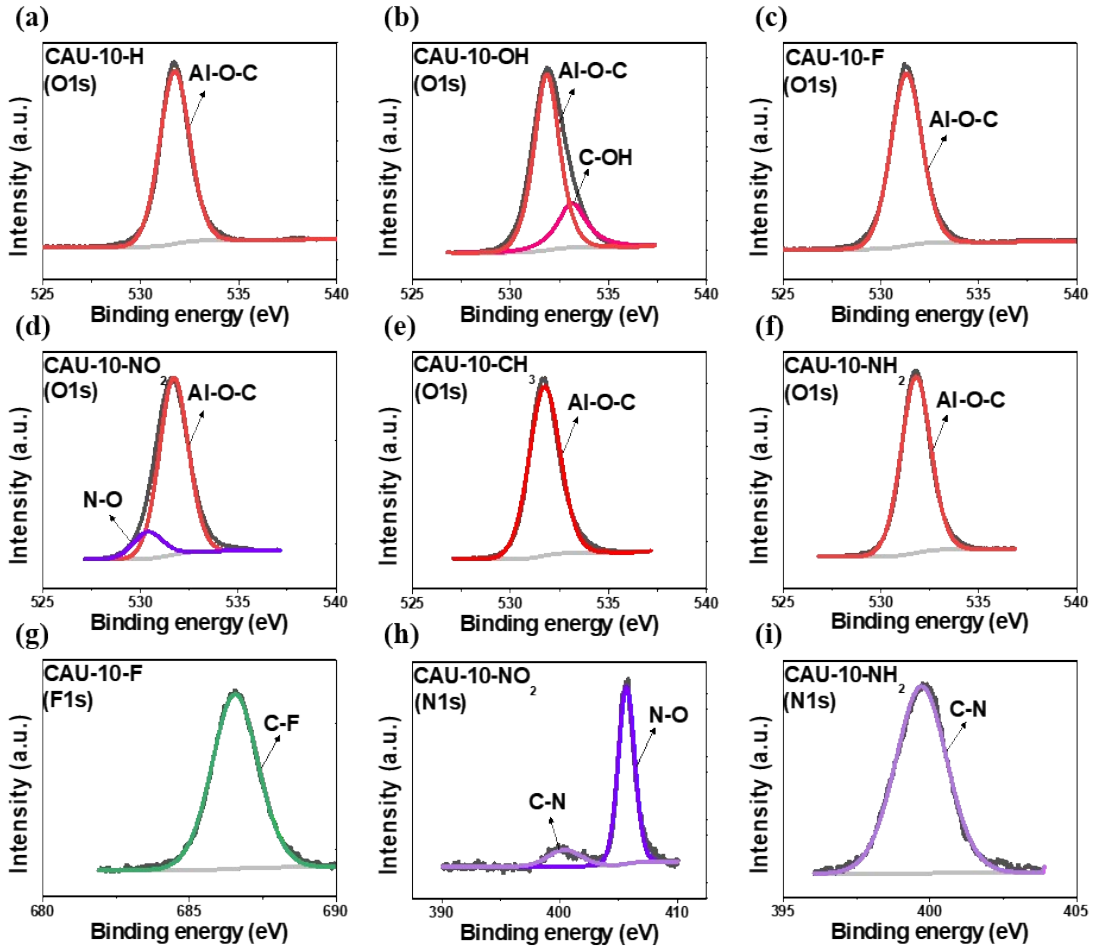

Fig. S5 O1s X-ray photoelectron spectroscopy (XPS) spectrum of (a) CAU-10-CH_3, (b) CAU-10-OH, (c) CAU-10-F, (d) CAU-10-NO_2, (e) CAU-10-CH_3, and (f) CAU-10-NH_2. (g) F1s spectrum of CAU-10-F, and N1s spectrum of (h) CAU-10-NO_2, (i) CAU-10-NH_2.

Table S4. Summarization of binding energy of XPS

Spectra	Assignment	Binding energy (eV)					
		CAU-10-H	CAU-10-OH	CAU-10-F	CAU-10-NO_2	CAU-10-NH_2	CAU-10-CH_3
C_{1S}	C=C, C-C	284.4	284.5	284.4	284.5	284.4	284.4
	O-C=O	288.6	288.7	288.7	288.5	288.5	288.6
	C-OH	-	286.3	-	-	-	-
	C-F	-	-	286.5	-	-	-
	C-N	-	-	-	285.9	285.7	-
	C-CH_3	-	-	-	-	-	284.9
O_{1S}	Al-O-C	531.7	531.8	531.3	531.8	531.8	531.8
	C-OH	-	533.1	-	-	-	-
	N-O	-	-	-	530.4	-	-
F_{1S}	C-F	-	-	686.5	-	-	-
N_{1S}	C-N	-	-	-	400.1	399.8	-
	N-O	-	-	-	405.6	-	-

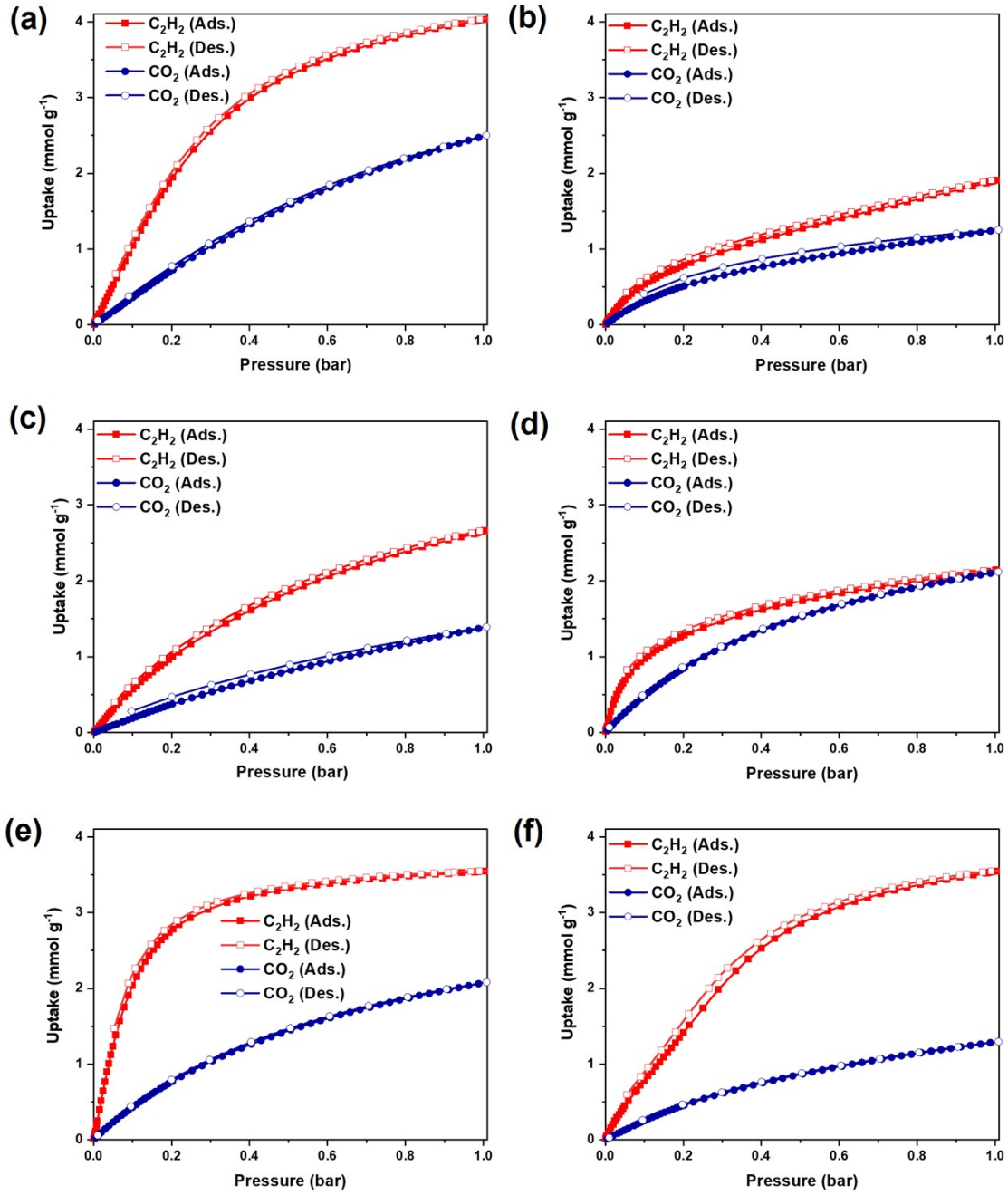

Fig. S6 C_2H_2 and CO_2 single component adsorption and desorption isotherms collected at 25 °C for CAU-10-X ((a) X=H (b) X=OH (c) X=F (d) X= NO_2 (e) X=NH_2 (f) X=CH_3. The adsorption data for C_2H_2 and CO_2 are shown in red square and blue circle whereas adsorption data for C_2H_2 and CO_2 are shown in empty red square and empty blue circle, respectively.

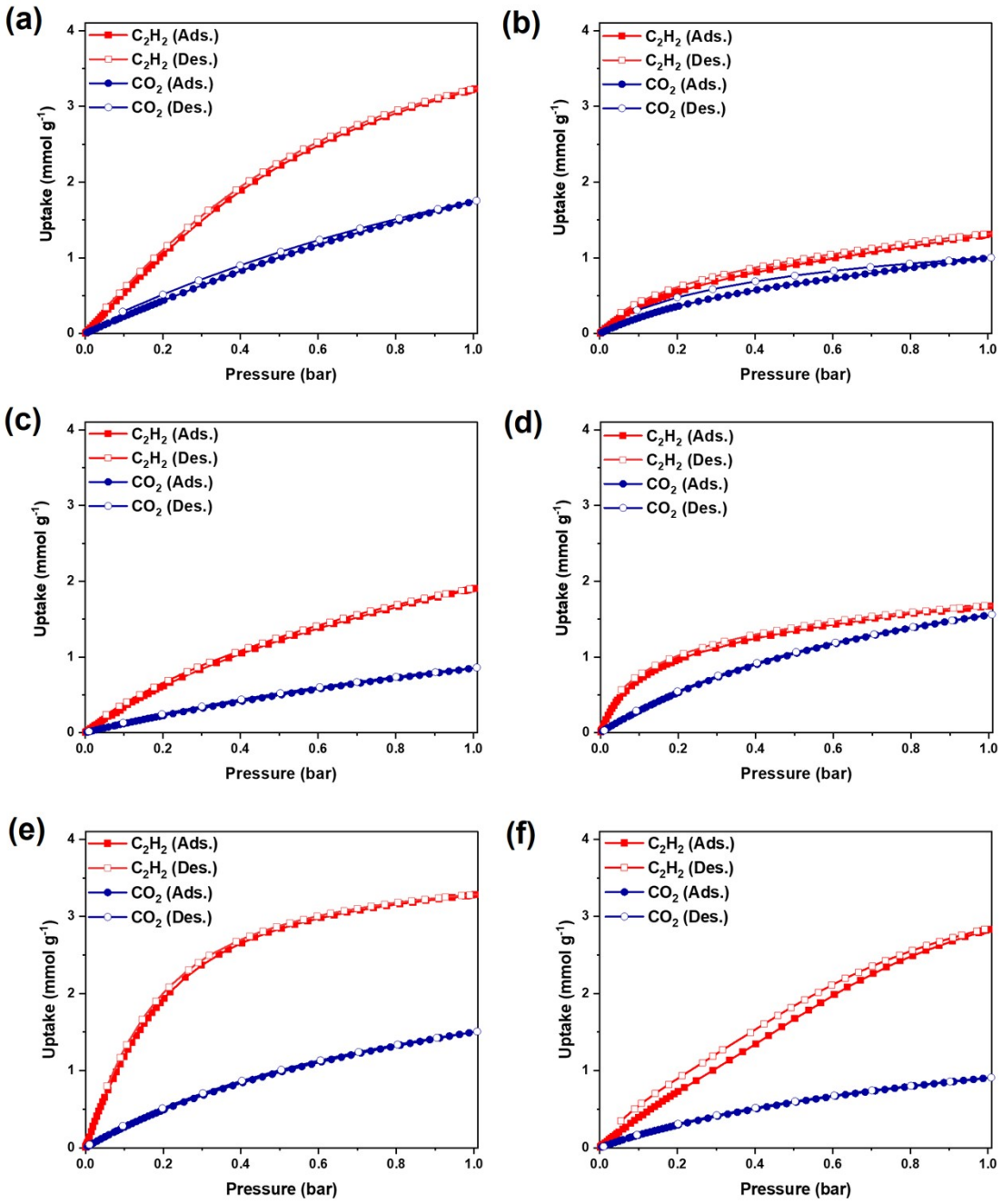

Fig. S7 C_2H_2 and CO_2 single component adsorption and desorption isotherms collected at 40 °C for CAU-10-X ((a) X=H (b) X=OH (c) X=F (d) X= NO_2 (e) X=NH_2 (f) X=CH_3. The adsorption data for C_2H_2 and CO_2 are shown in red square and blue circle whereas adsorption data for C_2H_2 and CO_2 are shown in empty red square and empty blue circle, respectively.

Isosteric enthalpy of adsorption:

The Q_{st} value was calculated from the isotherm collected at two different temperatures (25 ℃, and 40 ℃) by Eq. (1) and (2):

$$ln\,P = \ln N + \frac{1}{T}\sum_{i=0}^{m} a_i N^i + \sum_{i=0}^{n} b_i N^i \qquad (1)$$

$$Q_{st} = -R\sum_{i=0}^{m} a_i N^i \qquad (2)$$

where P is pressure (kPa), N is adsorbed quantity (mmol g^{-1}), T is temperature (K), R is universal gas constant (8.314 J mol^{-1} K^{-1}), ai and bi are virial coefficients, and m and n represent the number of coefficients required to adequately fit the isotherm.

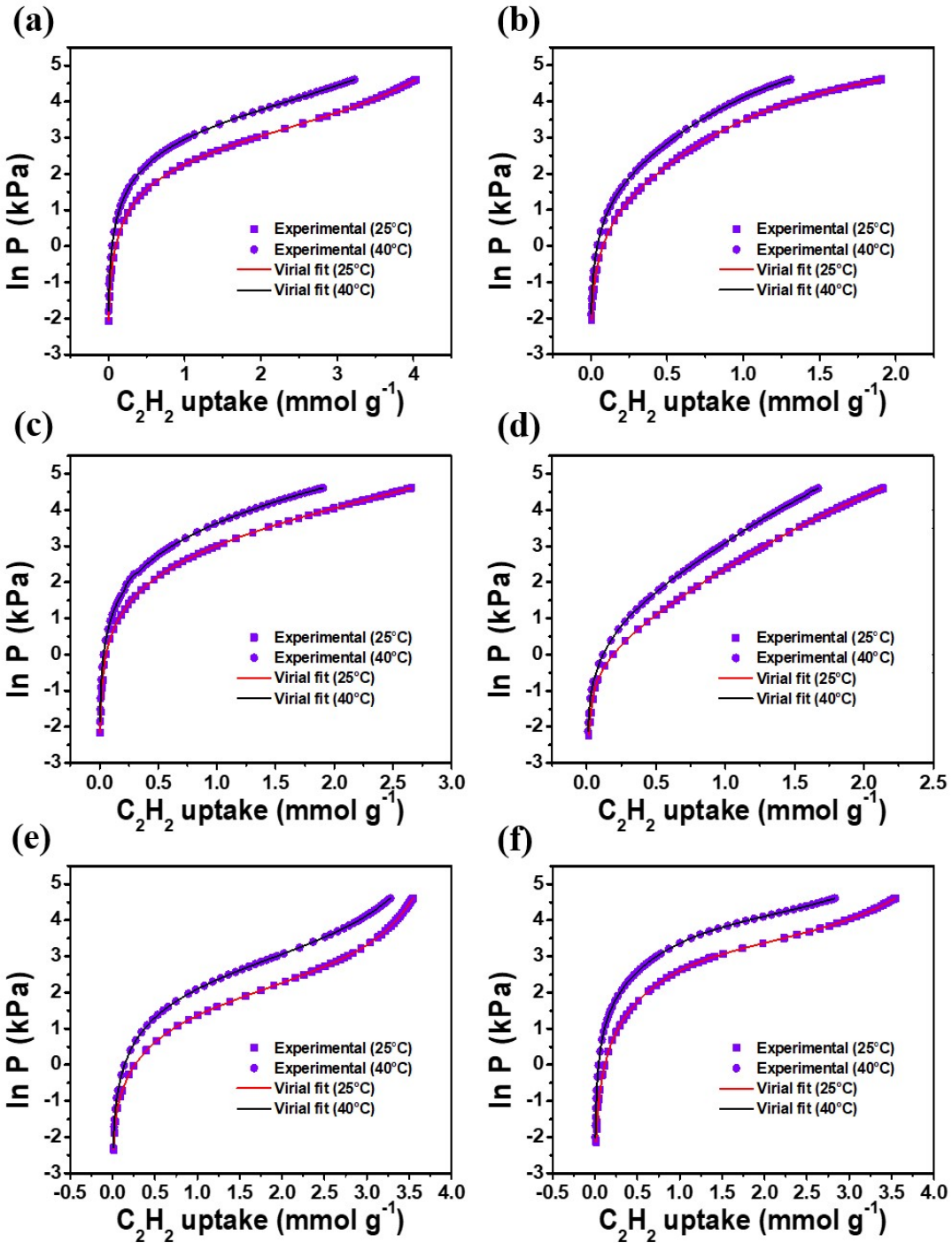

Fig. S8 Virial analysis fit for C_2H_2 adsorption isotherm of (a) CAU-10-H (b) CAU-10-OH (c) CAU-10-F (d) CAU-10-NO_2 (e) CAU-10-NH_2 (f) CAU-10-CH_3.

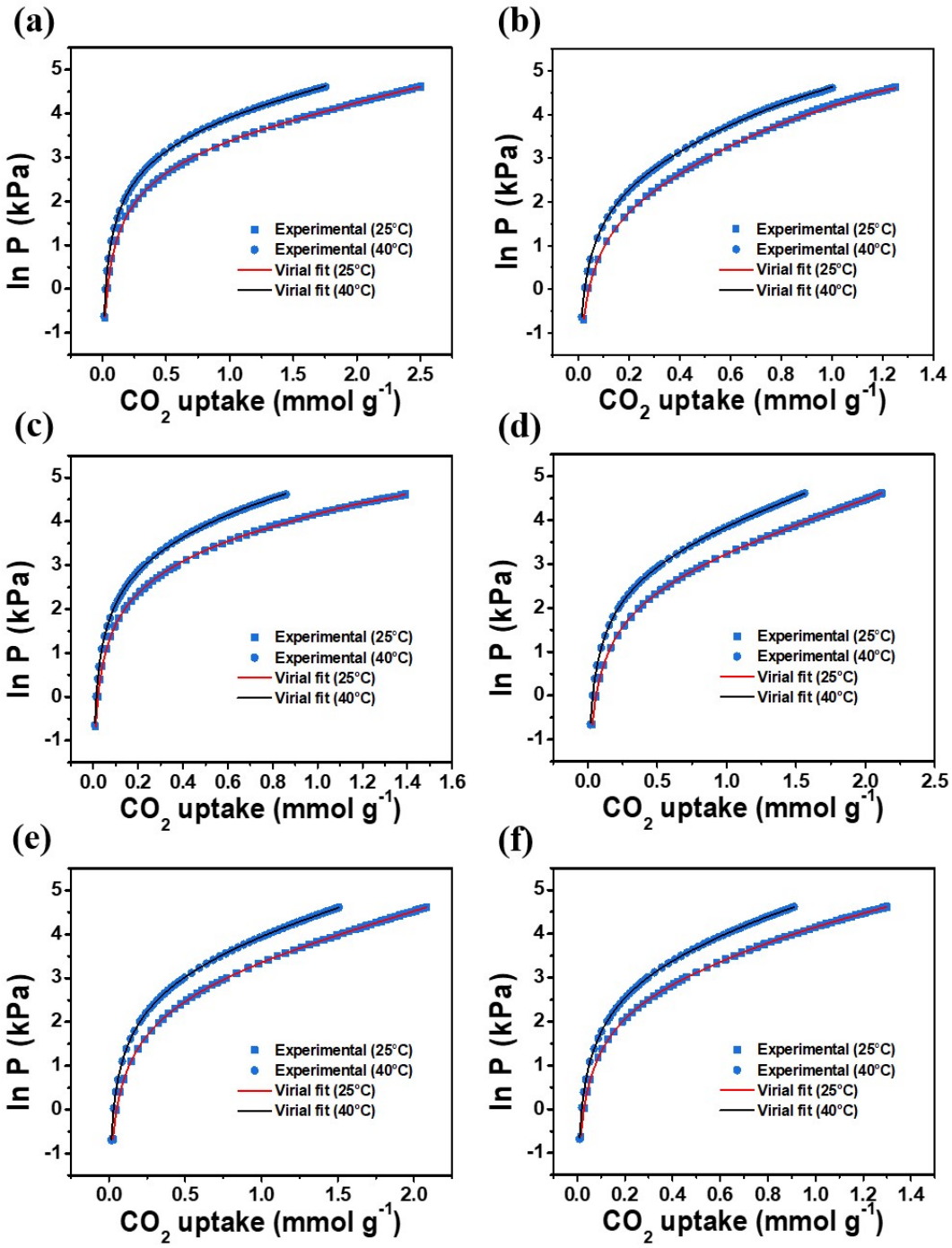

Fig. S9 Virial analysis fit for CO_2 adsorption isotherm of (a) CAU-10-H (b) CAU-10-OH (c) CAU-10-F (d) CAU-10-NO_2 (e) CAU-10-NH_2 (f) CAU-10-CH_3

Table S5. Summary of the fitted parameters of virial equation for C_2H_2 and CO_2 adsorption isotherms of CAU-10-X (X=H, OH, F) at 25 ℃ and 40 ℃

Parameters	CAU-10-H		CAU-10-OH		CAU-10-F	
	C_2H_2	CO_2	C_2H_2	CO_2	C_2H_2	CO_2
a0*	-3825.5091	-2918.8160	-3678.0487	-3466.5927	-3343.6253	-2761.0144
a1*	-1446.1882	-202.5473	-2715.7488	1007.7891	-959.1248	-1053.5855
a2*	3021.5922	-826.9571	13712.1738	-1615.5956	1936.7541	-4200.4985
a3*	-3507.7955	1521.5206	-32761.6218	4104.1751	-3214.5999	14129.9661
a4*	2122.7464	-1440.0202	41769.2087	-4100.1559	2892.7098	-25097.2241
a5*	-691.0147	736.8914	-29074.0745	632.5016	-1431.5691	24211.4364
a6*	114.8099	-192.5243	10381.9389	1348.3259	365.7205	-11950.9364
a7*	-7.6330	20.1191	-1485.9514	-602.6364	-37.6005	2359.7277
b0*	15.5939	13.0488	15.3147	14.7315	14.1439	13.0910
b1*	0.8691	1.4001	1.0864	-1.5057	1.5851	5.7111
R^2	0.9972	0.9999	0.9985	0.9999	0.9998	0.9999

Table S6. Summary of the fitted parameters of virial equation for C_2H_2 and CO_2 adsorption isotherms of CAU-10-X (X=NO_2, NH_2, CH_3) at 25 ℃ and 40 ℃

Parameters	CAU-10-NO_2		CAU-10-NH_2		CAU-10-CH_3	
	C_2H_2	CO_2	C_2H_2	CO_2	C_2H_2	CO_2
a0*	-2926.1564	-3507.3415	-3272.6830	-3277.9331	-6110.3536	-2718.8771
a1*	-2785.1598	-81.6616	-1939.5516	-258.8105	578.1891	-923.7776
a2*	4596.5364	-1226.0512	3387.6092	-626.8593	774.2731	-3550.7733
a3*	-7698.2057	2424.3869	-4158.9988	1226.2222	-1026.2931	11984.3001
a4*	7586.8085	-2572.7971	2690.8314	-1284.0084	624.6120	-21359.9167
a5*	-4283.1972	1518.3711	-940.7007	749.4177	-195.5274	20826.1608
a6*	1276.5165	-466.3159	167.9460	-228.3300	30.4581	-10457.6838
a7*	-155.4574	58.0318	-11.9373	28.3008	-1.8396	2111.7774
b0*	11.8150	14.5365	12.8573	13.9329	22.7141	12.5976
b1*	5.2846	1.6200	2.2577	1.7364	-2.2758	5.2636
R^2	0.9998	1.0000	0.9992	1.0000	0.9992	1.0000

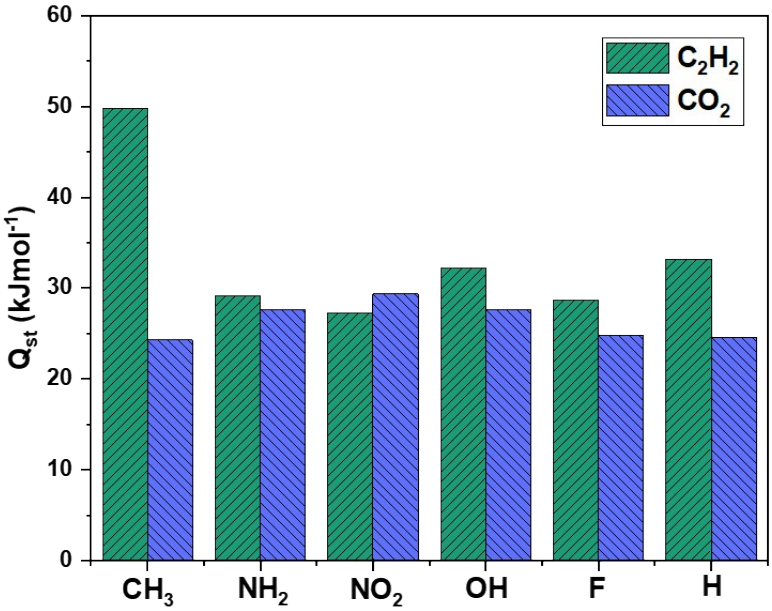

Fig. S10 Comparison of the Q_{st} at zero-coverage for C_2H_2 and CO_2 on functional group on CAU-10(Al)

Prediction of IAST selectivity

Myers and Prausnitz developed the ideal adsorbed solution theory (IAST) to predict the adsorption equilibria in multi-component gas mixture adsorption. The adsorption parameters calculated using the DSLF equation were used for the calculation of the IAST selectivity, as expressed in Eq. (S):

$$S = \frac{X_1}{X_2} \times \frac{Y_2}{Y_1}$$

where X_1 and X_2 are the mole fractions of the adsorbed C_2H_2 and CO_2, respectively, while Y_1 and Y_2 are the partial pressures of the C_2H_2 and CO_2 gas mixture.

Fitting of model equation of single component isotherms

The single-component C_2H_2 and CO_2 adsorption isotherms of CAU-10-X (X=H, OH, F, NO_2, NH_2, CH_3) were fitted using the dual-site Langmuir Freundlich (DSFL) model to obtain the best fitting result by IAST++ software. The fit graphs provided by software are given in Fig. S4& S5. The isotherm parameter obtained from fitting is presented in Table S4.

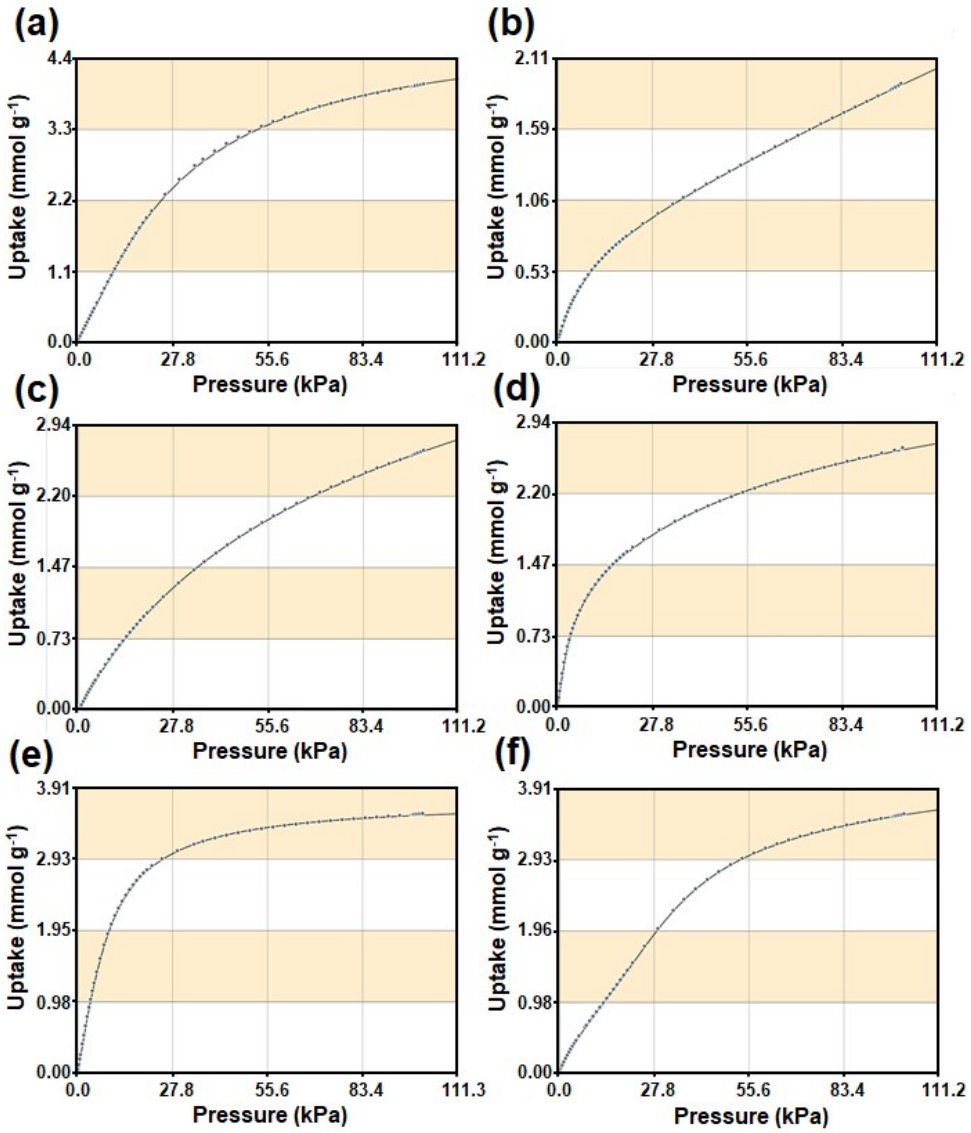

Fig. S11 Results for the fitting of experimental C_2H_2 isotherm curves obtained at 25°C for CAU-10-X with Dual-site Langmuir Freundlich model where grey dot is experimental data and black line is fitting for DSLF model (a) CAU-10-H (b) CAU-10-OH (c) CAU-10-F (d) CAU-10-NO_2 (e) CAU-10-NH_2 (f) CAU-10-CH_3.

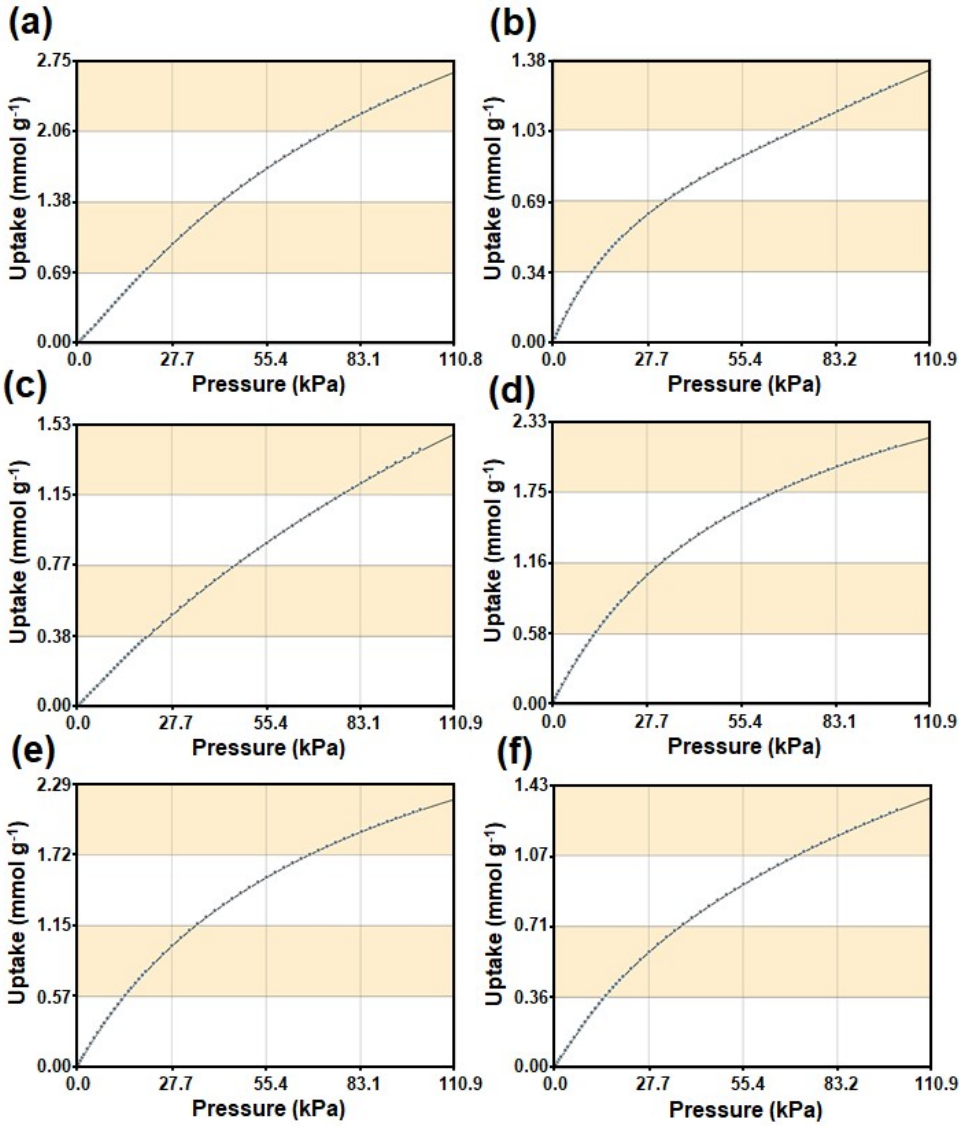

Fig. S12 Results for the fitting of experimental CO_2 isotherm curves obtained at 25°C for CAU-10-X with Dual-site Langmuir Freundlich model where grey dot is experimental data and black line is fitting for DSLF model (a) CAU-10-H (b) CAU-10-OH (c) CAU-10-F (d) CAU-10-NO_2 (e) CAU-10-NH_2 (f) CAU-10-CH_3.

Table S7. Dual-site Langmuir fit parameter for CAU-10-X at 25 °C

Sample	Dual-site Langmuir Freundlich Model							
	Gas	q_1 (mmol/g)	k_1 (1/kPa)	n_1	q_2 (mmol/g)	k_2 (1/kPa)	n_2	R^2
CAU-10-H	C_2H_2	4.5150	3.64E^{-2}	1.3756	0.1568	0.5677	1.3434	0.9999
	CO_2	1.4918	0.0188	1.3996	6.6029	0.0024	0.8897	0.9999
CAU-10-OH	C_2H_2	9.4136	0.0017	1.1198	0.7779	0.1211	1.0982	0.9999
	CO_2	1.5546	0.2367	0.9603	0.5165	0.0082	3.7444	0.9999
CAU-10-F	C_2H_2	4.6789	0.0130	0.9797	5.92E^{-18}	5.5595	1.3887	0.9999
	CO_2	4.5358	0.0043	0.9910	4.02E^{-17}	54.2806	39.7543	0.9999
CAU-10-NO_2	C_2H_2	2.4088	0.0129	0.9117	0.7923	0.3160	1.3193	0.9999
	CO_2	3.3706	0.0164	0.9885	0.0293	0.0107	8.9960	1.0000
CAU-10-NH_2	C_2H_2	3.5567	0.1161	1.1926	0.1560	0.1202	3.8672	0.9999
	CO_2	3.7883	0.0098	0.9381	0.2336	0.0361	1.3167	1.0000
CAU-10-CH_3	C_2H_2	3.4925	0.0245	0.9146	1.1375	0.0323	3.3455	0.9999
	CO_2	3.2390	0.0052	0.9033	0.1384	0.0628	1.7869	1.0000

Table S8. Comparative C_2H_2 adsorption performance of MOFs at 25 °C and 1 bar with no open metal sites from literature.

Materials	C_2H_2 uptake (mmol g^{-1})	CO_2 uptake (mmol g^{-1})	C_2H_2/CO_2 uptake ratio	C_2H_2/CO_2 Selectivity	Ref.
MIL-160	8.5	4	2.1	10	J. Am. Chem. Soc. 2022, 144, 1681−1689
CAU-23	5.3	3.2	1.6	3.8	J. Am. Chem. Soc. 2022, 144, 1681−1689
MUF-17	3	2.5	1.2	6	Chem. Mater., 2019, 31, 4919–4926
JCM-1	3.3	2.5	1.3	13.6	Angew. Chem., Int. Ed., 2018, 57, 7869–7873
FJU-90A	8	4.5	1.7	4.3	J. Am. Chem. Soc., 2019, 141, 4130–4136
FJU-36A	2.3	1.5	1.5	2.8	Inorg. Chem., 2018, 57, 12961–12968
ZJNU-13	5.2	3.9	1.3	5.6	ACS Appl. Nano Mater., 2020, 3, 2911–2919
ZJU-195A	9.5	4.6	2	4.7	ACS Sustainable Chem. Eng., 2019, 7, 2134–2140
NBU-8	8.1	2.2	3.6	5.4	Inorg. Chem., 2020, 59, 13005–13008
ZJNU-8	4.1	3.7	1.1	4.5	Eur. J. Inorg. Chem., 2020, 17, 1683–1689
UPC-110	3.2	1.1	2.9	5.1	ACS Sustainable Chem. Eng.,2019, 7, 2134–2140
Co(btzip)(H_2btzip)	3.8	3.2	1.1	2.45	ACS Appl. Mater. Interfaces, 2020, 12, 41785–41793
ZJUT-2	3.4	2.1	1.6	10	Chem. Commun., 2019, 55, 11354–11357
CAU-10-H	4	2.5	1.6	3.1	This work
CAU-10-OH	1.9	1.3	1.1	2.1	This work
CAU-10-F	2.7	1.4	1.9	3.2	This work
CAU-10-NO_2	2.1	2.1	1	2.1	This work
CAU-10-NH_2	3.5	2.1	1.6	8.4	This work
CAU-10-CH_3	3.5	1.3	2.7	6.5	This work

Diffusion time constant:

The diffusion time constant is denoted by the ratio D (D_c/r_c^2). From the following micropore diffusion model equation, it can be further derived :

$$\frac{M_T}{M_E} = \frac{6}{r_c}\sqrt{\frac{D_c T}{\pi}}$$

where M_E represents equilibrium gas uptake. The gas uptake at time T is denoted by M_T, the equivalent spherical particle's radius is represented by r_c, and the inter-crystalline diffusivity of gas molecules in porous media is indicated by D_c. By multiplying the square of the slope (M_T/M_E plotted against $T^{1/2}$) by $\pi/36$, one can determine D.

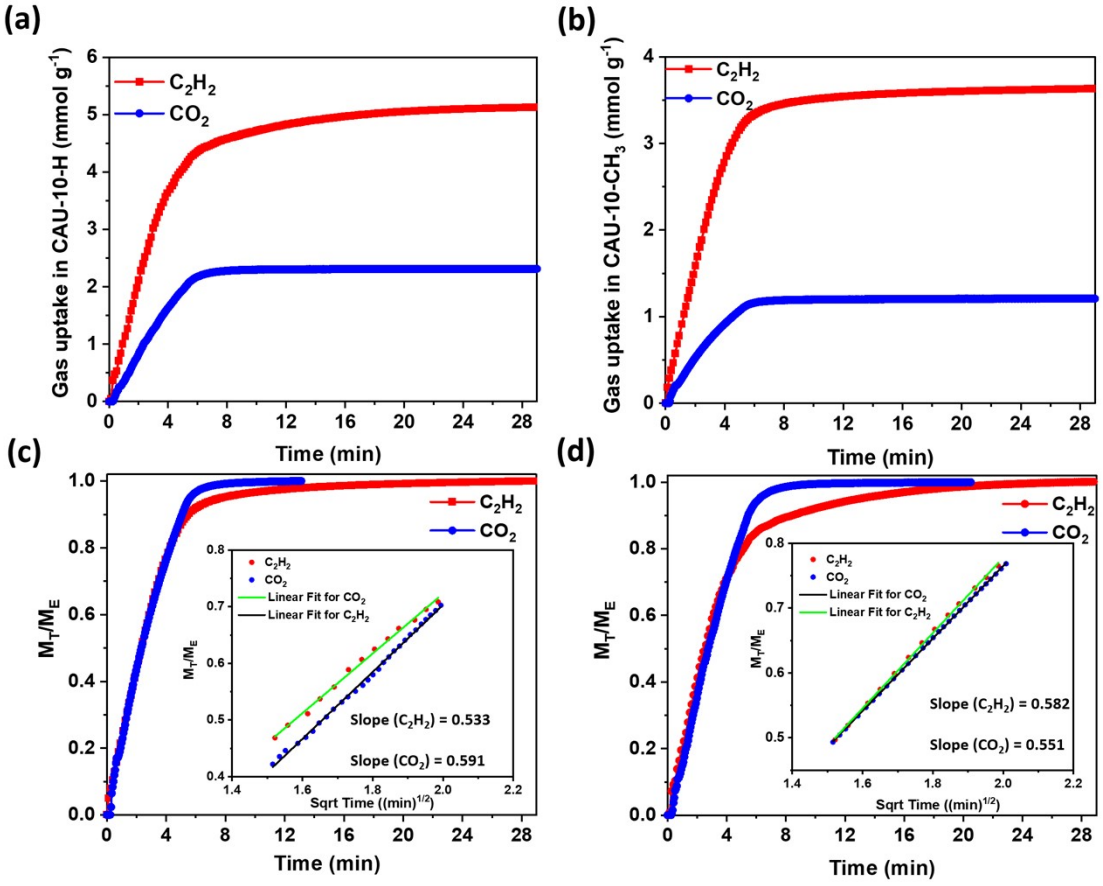

Fig. S13 Adsorption kinetic diagrams of C_2H_2 and CO_2 adsorption upto 1 bar at 25 °C on (a) CAU-10-H (b) CAU-10-CH_3. Normalized scale plots with respect to equilibrium uptake of C_2H_2 and CO_2 upto 1 bar at 25 °C for (c) CAU-10-H (d). CAU-10-CH_3. Fitting for time dependent adsorption data for diffusion time constant determination as inset figure in (c) CAU-10-H (d) CAU-10-CH_3.

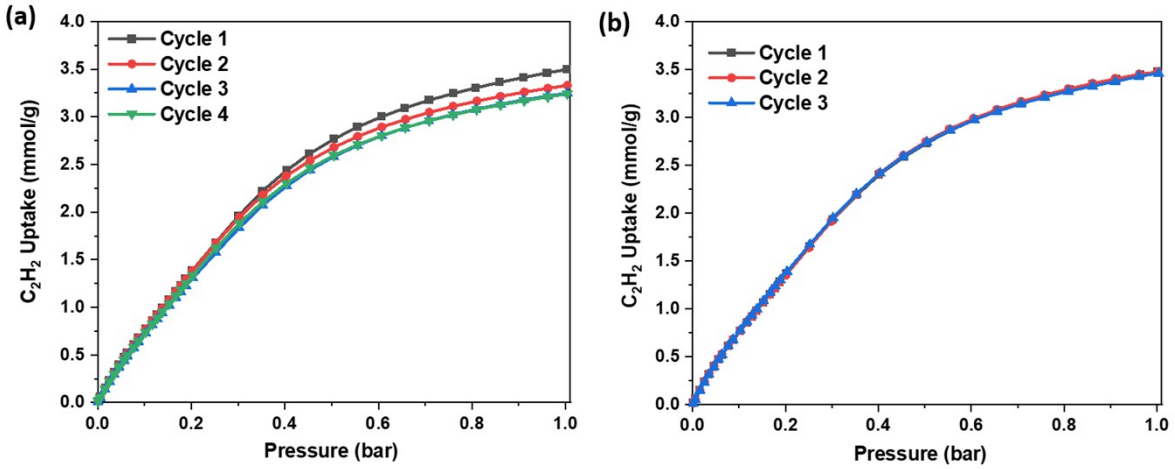

Fig. S14 (a) Repeated single-gas (C_2H_2) adsorption and desorption cycles for CAU-10-CH_3 by employing desorption using vacuum (5 x 10^{-4} Torr). (b) Repeated single-gas (C_2H_2) adsorption and desorption cycles for CAU-10-CH_3 by employing desorption under vacuum (5 x 10^{-4} Torr) at a temperature of 200 °C.

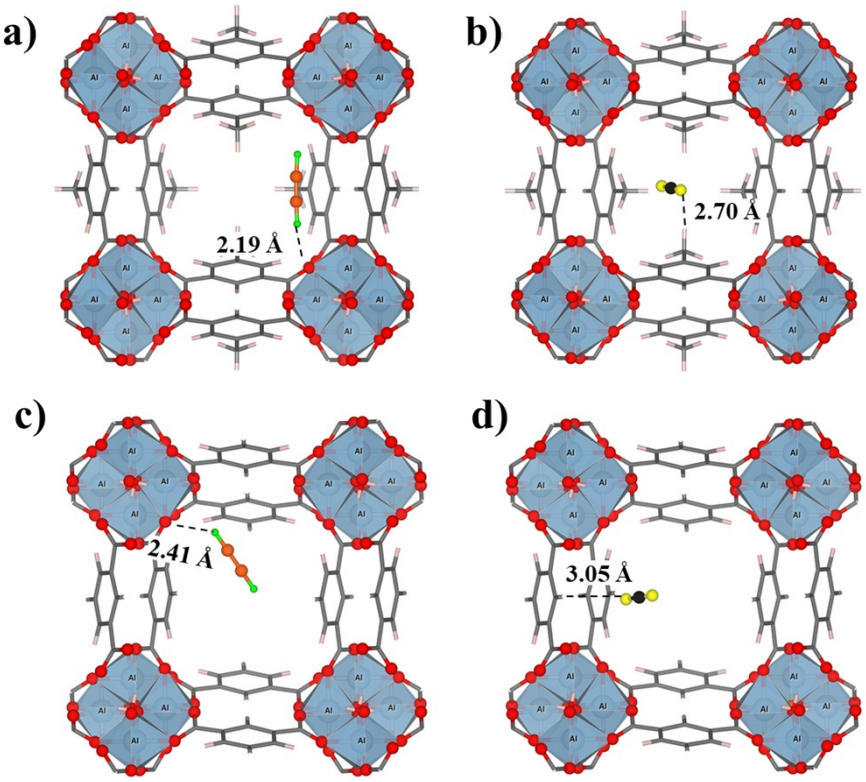

Fig. S15 DFT-optimized geometries of (a,c) C_2H_2 and (b,d) CO_2 adsorption on CAU-10-H (bottom) and CAU-10-CH_3 (top). Color code: blue (Al), red (O), gray (C), white (H), yellow (O of CO_2), black (C of CO_2), orange (C of C_2H_2), and green (H of C_2H_2).

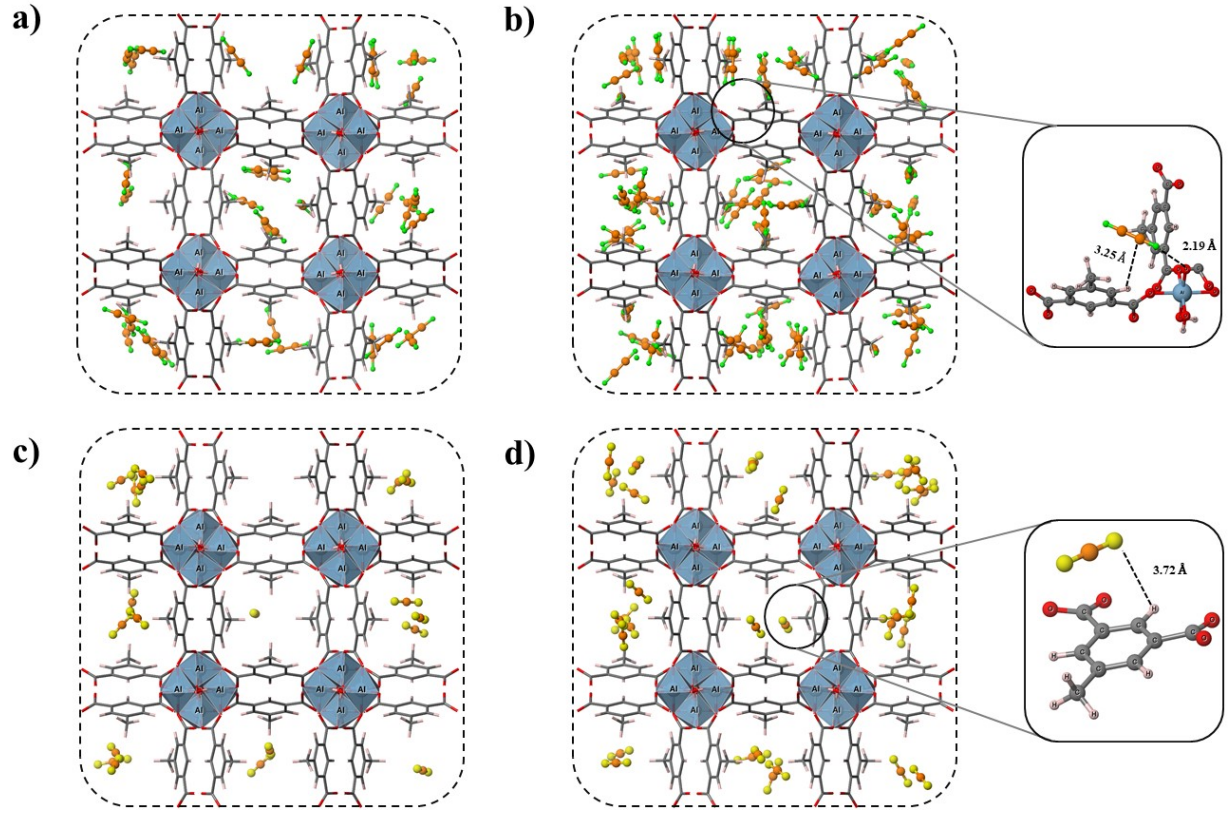

Fig. S16 (a,b) C_2H_2 and (c,d) CO_2 single component Monte Carlo simulation snapshots of CAU-10-CH_3 calculated at 25 °C with 0.2 bar (left) and 1 bar (right). Color code: blue (Al), red (O), gray (C), white (H), yellow (O of CO_2), orange (C of CO_2 and C_2H_2), and green (H of C_2H_2).

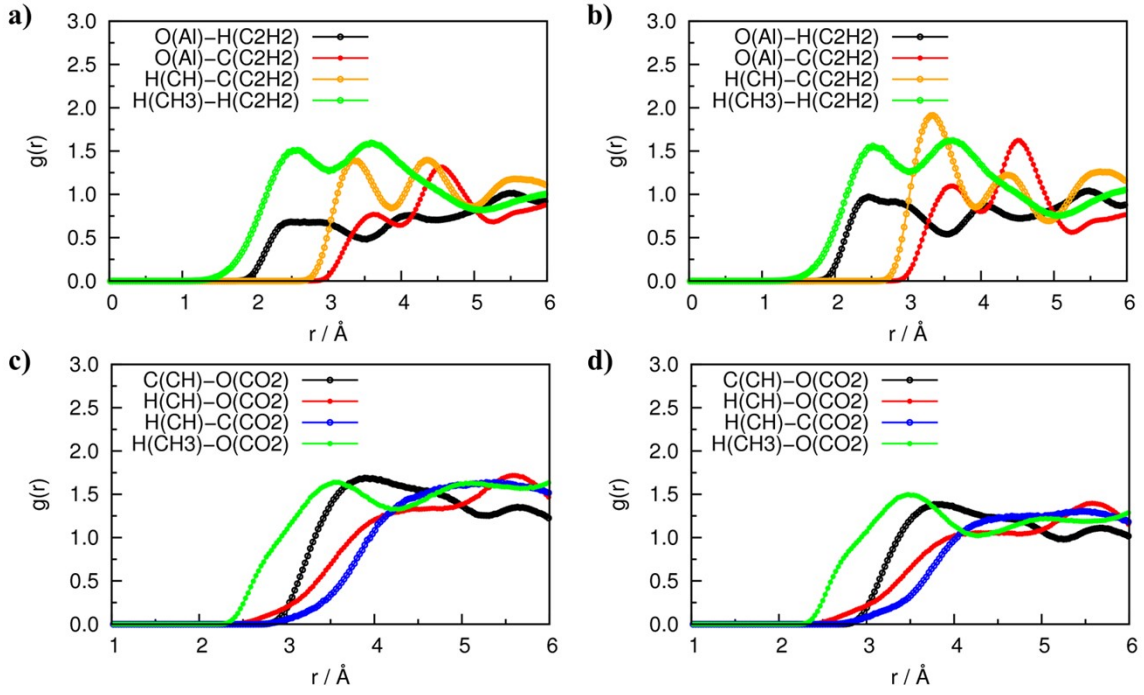

Fig. S17 (a,b) C_2H_2 and (c,d) CO_2 Radial distribution functions for representative atom pairs related to CAU-10-CH_3 calculated from the Monte Carlo simulations at 25°C with 0.2 bar (left) and 1 bar (right).

Force Field validation

We initially selected CAU-10-H as the benchmark MOF framework to validate the selected force field parameters and atomic partial charges to describe the interactions between the two guest molecules and the host framework.

We first use UFF force field to describe the Lennard-Jones parameters for the atoms of the MOF framework, CO_2 was described by the well-established EPM2 model and C_2H_2 was represented by the model reported by Fisher et al. First, the interaction energy was computed through a MC simulation performed in the NVT ensemble for a single molecule per unit cell at 25°C. These energetic values were compared with the DFT interaction energy and the experimental Qst, as illustrated in **Fig. S18**. Notably, both the NVT simulation at 298 K and DFT calculations at 0 K show a reasonable accordance with the experimental Qst, indicating that CAU-10-H possesses a higher affinity for C_2H_2 compared to CO_2. Specifically, the DFT calculations evidence an interaction energy difference between C_2H_2 and CO_2 of 6.7 kJ/mol, while the simulated adsorption energy difference is 4.3 kJ/mol and the experimental isosteric enthalpy of adsorption difference is 9.20 kJ/mol.

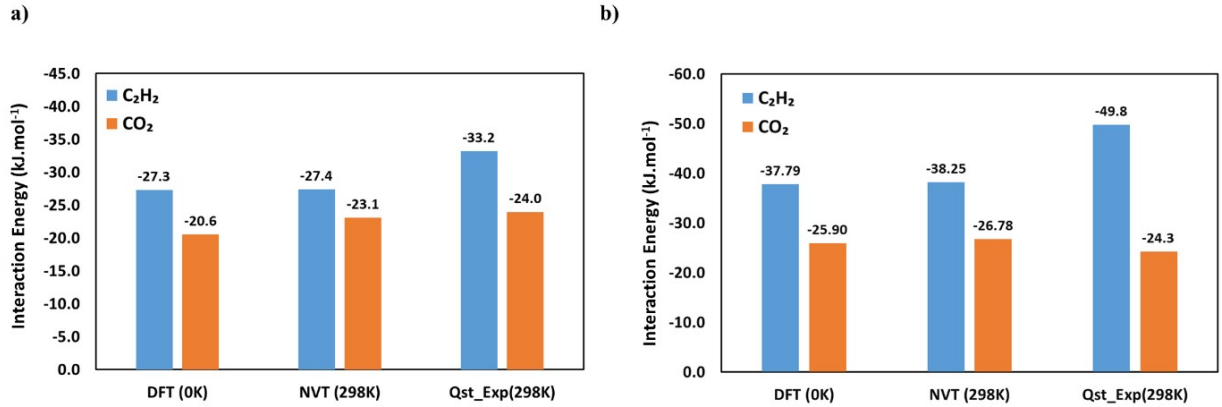

Fig. S18 Comparative calculated interaction energy of C_2H_2 and CO_2 on (a) CAU-10-H and (b) CAU-10-CH_3: DFT and NVT-Monte Carlo (25°C) alongside the experimental Qst value at 25 °C.

Subsequently, we computed the single-component C_2H_2 and CO_2 adsorption isotherms.

Remarkably, there is an excellent agreement observed between the simulated C_2H_2 adsorption isotherm at 25°C and the corresponding experimental data within the pressure range of 0-1 bar. However, regarding CO_2, the simulated adsorption isotherm is shown to overestimate the experimental results (**Fig. 6a**). To address this, additional testing was conducted by implementing different set of LJ parameters for the MOF atoms, including a full description of the LJ parameters by the Dreiding force field and a mixed one with Dreiding and UFF LJ parameters (i.e., the organic part is described by Dreiding and inorganic part by UFF). A comparison of the single-component isotherms of CO_2 using these different force fields is delivered in **Fig. S19a**. The analysis revealed that utilizing the mixed strategy UFF/Dreiding leads to a slightly better description of the experimental CO_2 adsorption isotherm than the use of pure UFF. Additionally, a comprehensive comparison of three different CO_2 models was conducted in the case of the LJ parameters of the MOF framework atoms described by UFF. The corresponding results illustrated in **Fig. S19b** indicate that the EPM2 model leads to a better description of the experimental data than the two other tested models.

When we used the same UFF force field to describe the LJ parameters of the CAU-10-CH_3 atoms, we managed to capture reasonably the CO_2 sorption isotherm especially the amount adsorbed at 1 bar as shown in Fig. 6b. This was not the case for C_2H_2 where only satisfactory agreement was obtained between the experimental and simulated adsorption isotherms at very low-pressure ranges (<0.2 bar- see **Fig. S21a**). At higher loading, the GCMC simulated C_2H_2 adsorption isotherm substantially deviated from the experimental data (Fig. S20a). We suspected that C_2H_2 molecules, especially at higher loadings, should approach the MOF framework more closely than the Monte Carlo simulations allow due the structural constraints posed by the bulky functional -CH_3 groups and the rigidity of the MOF framework considered in these calculations. To verify this assumption, AIMD simulations were considered to dynamically assess the distance between the carbon atoms of the functionalized CH_3 group and the adsorbed C_2H_2 molecules. Specifically, the AIMD simulations were performed for a loading of C_2H_2 corresponding to the adsorbed amount experimentally obtained at 1 bar (3.5 mmol/g), i.e. about 13 molecules per unit cell. Subsequently, the calculated interaction distances of carbon and hydrogen atoms of the CH_3 group and the C_2H_2 molecules. were considered to adjust the value of sigma in the force field (**Table S10**), while maintaining the other interactions treated by the set of initial LJ parameters. This fine-tuning strategy aimed to

better capture the spatial constraints and intermolecular interactions specific to the CAU-10-CH_3 structure, thus improving the accuracy of the adsorption predictions, particularly for C_2H_2 at varying pressures and loadings as shown in **Fig. S21a.**

The validation stage involves a comprehensive comparison between the results obtained from AIMD simulations and those predicted by force field MC simulations. The Radial Distribution Function (RDF) obtained from AIMD simulations, as illustrated in Supplementary **Fig. S20**, served as a reference point. Supplementary **Fig. S21** presents the RDF obtained at 1bar pressure, alongside a comparative analysis of the single-component isotherm for C_2H_2 adsorption, both with and without the LJ sigma correction, against the experimental data.

The agreement between the RDF predicted by the force field with the RDF obtained from AIMD simulations at various pressures further validated the accuracy of the refined force field in capturing the C_2H_2 molecular interactions within the CAU-10-CH_3 structure. C_2H_2 and CO_2 single component Monte Carlo simulation snapshots and RDF of of CAU-10-H calculated at 25 ^oC with 0.2 bar and 1 bar are presented as **Fig. S22** and **Fig. S23.**

Table S9. Cell parameters of the DFT-optimized CAU-10X (X = $^{-}$H, $^{-}CH_3$)

Structure	Loaded molecule	a(Å)	b(Å)	c(Å)	$\alpha \approx \beta \approx \gamma$	$Volume$(Å^3)
CAU-10-H	C_2H_2	21.49	21.49	10.18	90	4701.32
	CO_2	21.55	21.54	9.86	90	4576.89
CAU-10-CH_3	C_2H_2	21.61	21.59	10.20	90	4760.30
	CO_2	21.58	21.57	10.00	90	4654.80

Table S10. LJ Potential Parameters of Host and Guest Molecules

System	Atom	σ (Å)	$\varepsilon/k_B(K)$	Q
MOFs	Al	4.0081	0.0000	Cc
	C	3.4308	52.8389	
	H	2.5711	22.1420	
	H_OH	2.5711	0.0000	
	O	3.1181	30.1937	
Guest Molecules				
CO_2	C	2.7570	28.1290	0.6512
	O	3.0330	80.5070	$^{-}$0.3256
	O	3.0330	80.5070	$^{-}$0.3256
C_2H_2	C	3.8000	57.8754	$^{-}$0.2780
	C	3.8000	57.8754	$^{-}$0.2780
	H[a]	0.0000	0.0000	0.2780
	H[a]	0.0000	0.0000	0.2780
Defined interactions of C_2H_2 with CH_3 of CAU-10-CH_3				
C_H_3 $^{-}$ C_C_2H_2		3.0154	55.2999	

cc - All studied CAU-10-X structures atomic partial charges were derived from by applying the DDEC (Density Derived Electrostatic and Chemical charges) method using CHARGEMOL module. These charges have been incorporated into the CIF file provided. a - Hydrogen atoms in acetylene were represented as non-interacting atoms.

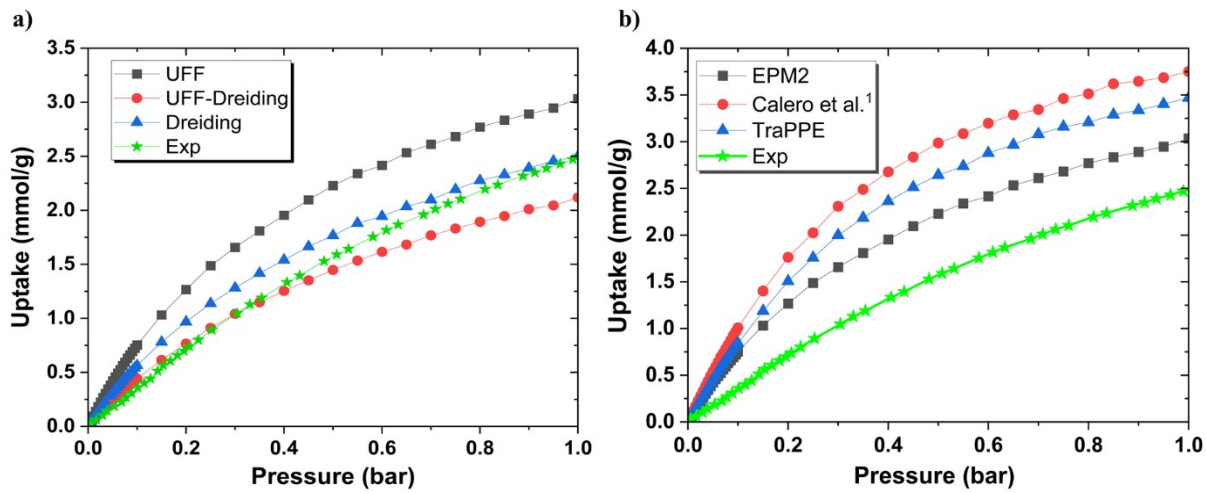

Fig. S19 GCMC-predicted single component CO_2 adsorption isotherms for CAU-10-H computed using (a) different force fields for the MOF framework with EPM2 model for CO_2 and (b) different CO_2 FF models for the MOF framework treated by UFF in the pressure range 0-1 bar at 25°C.

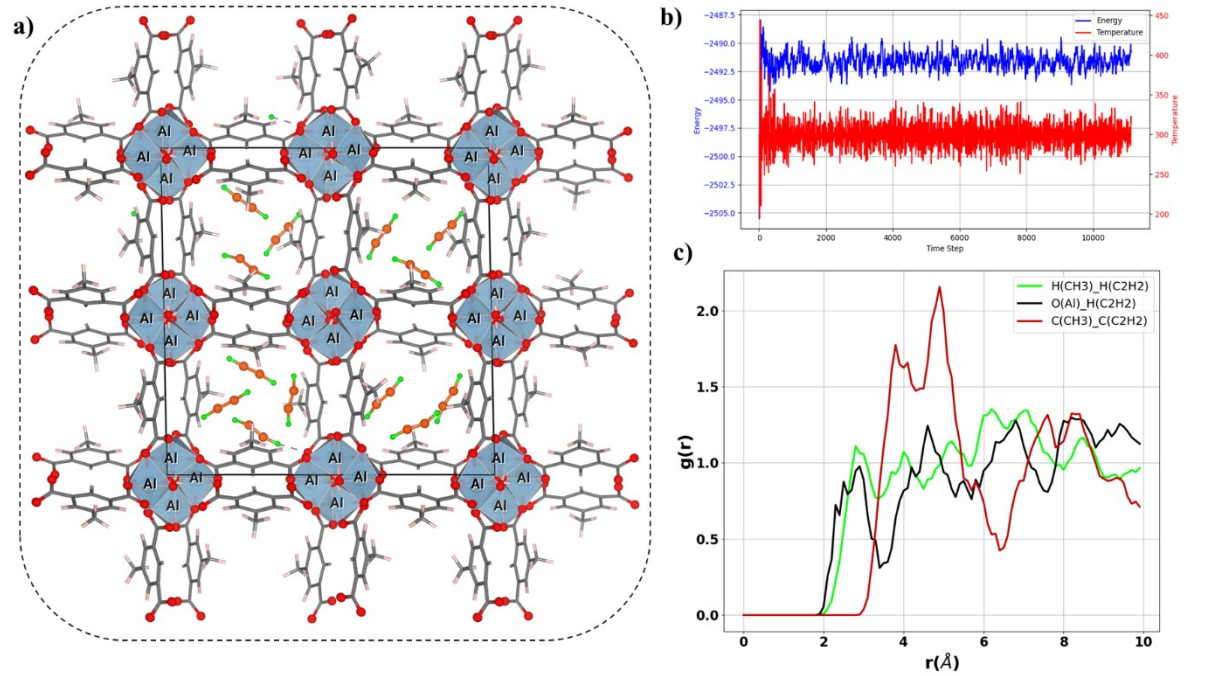

Fig. S20 AIMD simulations depicting the interaction of C_2H_2 molecules within CAU-10-CH_3 (a) a representative snapshot captured after 20 ps AIMD simulation run with 13 molecules per unit cell (corresponds to 3.5 mmol/g obtained experimentally at 1 bar), (b) Total energy and temperature variations throughout the 20 ps AIMD trajectory, and c) RDF analysis for the most representative MOF-C_2H_2 atom pairs averaged over the 20ps AIMD run.

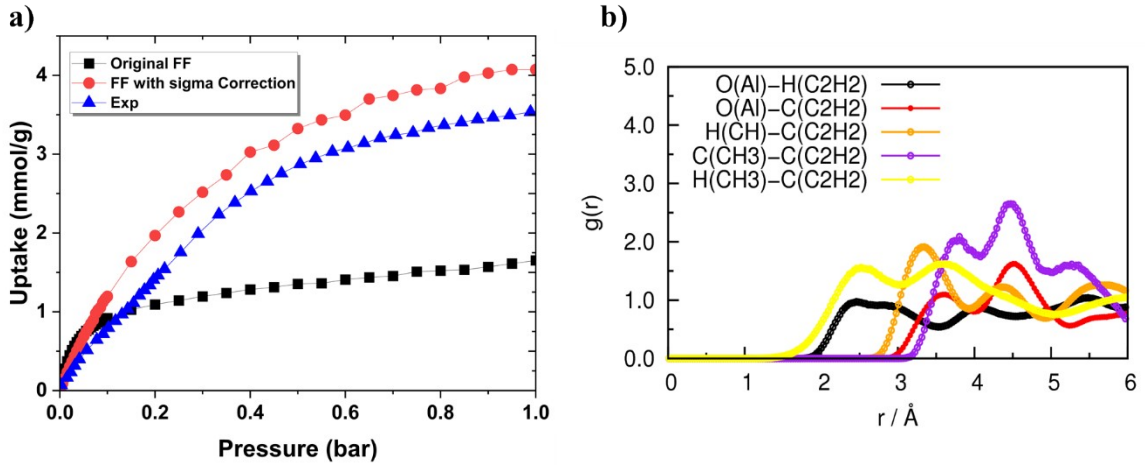

Fig. S21 (a) Comparison of the GCMC-predicted single component C_2H_2 adsorption isotherm for CAU-10-CH_3 with and without sigma correction for the C_2H_2-CH_3 atom pairs alongside the experimental data, and (b) RDF analysis for the most representative MOF-C_2H_2 atom pairs obtained at 1 bar for the scenario where sigma correction was applied.

.

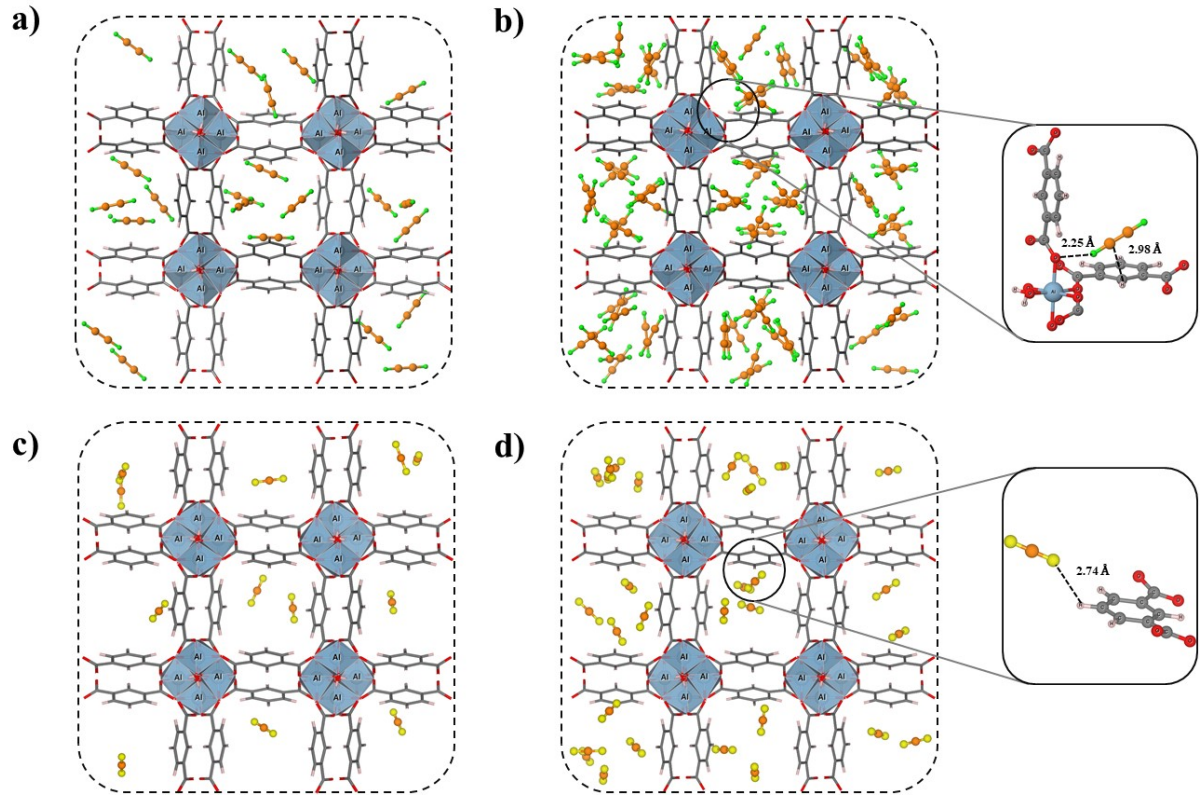

Fig. S22 (a,b) C_2H_2 and (c,d) CO_2 single component Monte Carlo simulation snapshots of CAU-10-H calculated at 25°C with 0.2 bar (left) and 1 bar (right). Color code: blue (Al), red (O), gray (C), white (H), yellow (O of CO_2), orange (C of CO_2 and C_2H_2), and green (H of C_2H_2).

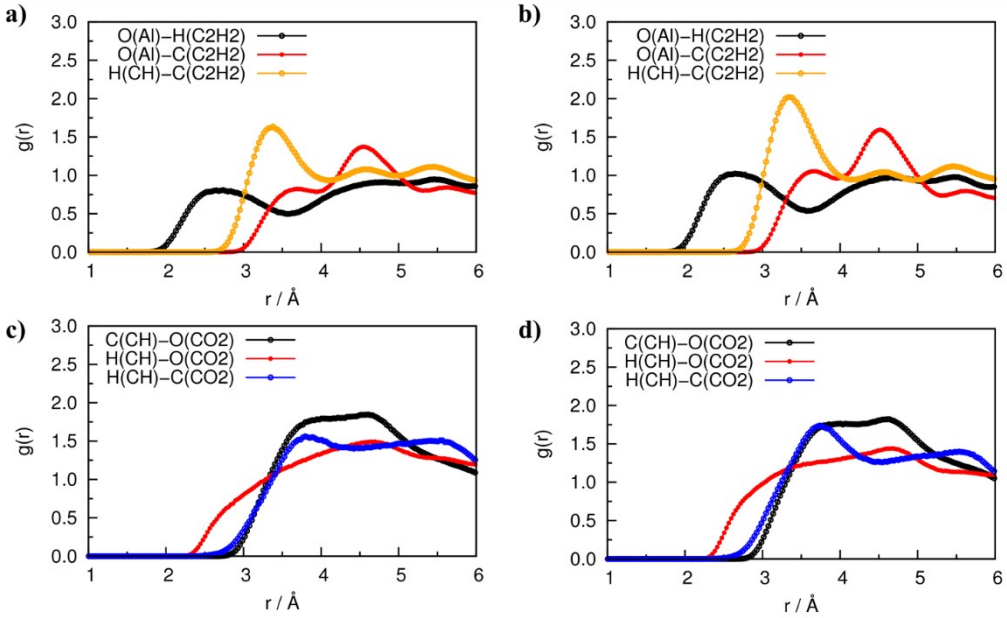

Fig. S23 (a,b) C_2H_2 and (c,d) CO_2 RDF of CAU-10-H calculated from the MC simulations at 25°C with 0.2 bar (left) and 1 bar (right).

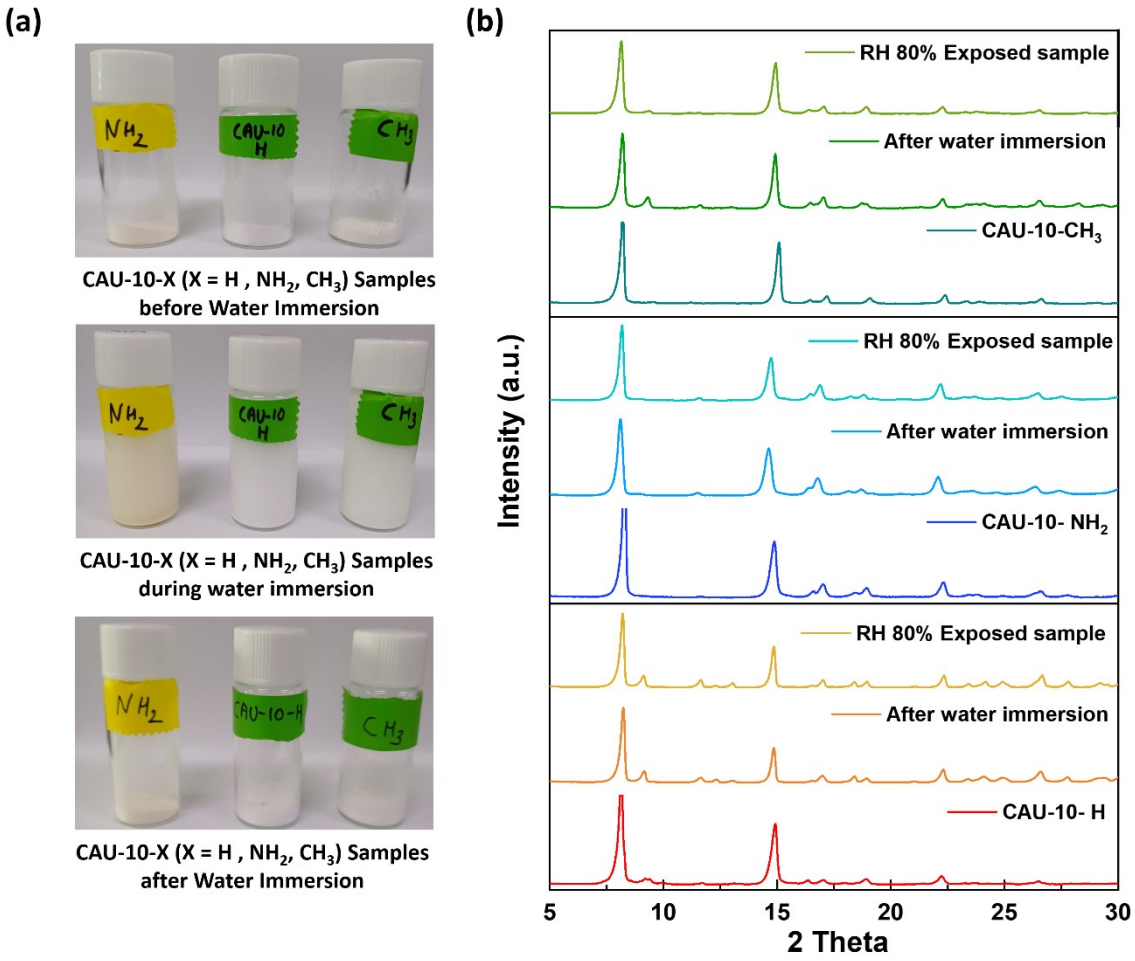

Fig. S24 (a) Showing CAU-10-NH_2, CAU-10-H, and CAU-10-CH_3 samples before water immersion,(TOP) under water (middle) and dried sample (below).(b) PXRD comparison of as-synthesized, dried after 72 hour water immersion and after 72 hour exposure to RH-80 for CAU-10-H, CAU-10-NH_2, and CAU-10-CH_3 samples.

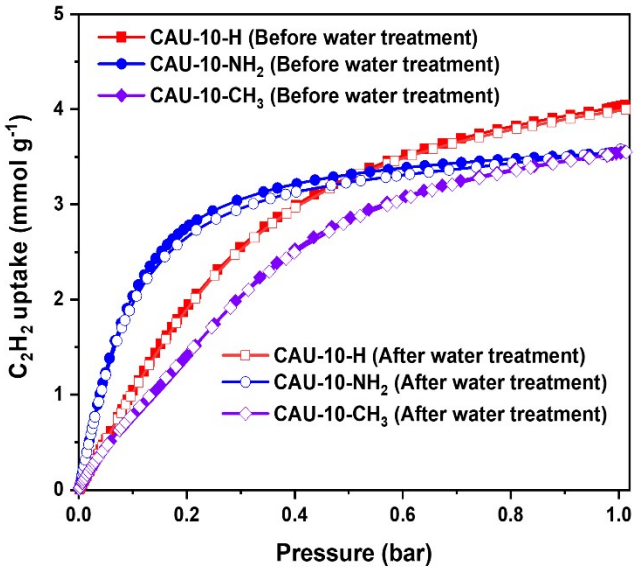

Fig. S25 Comparison of C_2H_2 gas adsorption capacity of before and after water treatment (72-hour water immersion) for CAU-10-H, CAU-10-NH_2, and CAU-10-CH_3 samples.

Experimental Section

Synthesis method of CAU-10

1 Synthesis of CAU-10-H

For CAU-10-H synthesis, $Al(NO_3)_3 \cdot 9H_2O$ (4.0 g) and isophthalic acid (2.0 g) were dissolved in H_2O (36 ml) and DMF (10 ml), respectively, under stirring. The mixture was placed in a 100 ml Teflon-lined steel autoclave and heated up to 135 ℃, and held for 12 h in a convection oven. After it was cooled to room temperature, the obtained solid was dispersed in EtOH and placed in a sonication water bath at 70 ℃ for 3 h. The mixture was then filtered and washed with EtOH. This purification procedure was repeated two times. Finally, the obtained solid was dried overnight at 100℃ under an air condition.

2 Synthesis of CAU-10-OH

CAU-10-OH was synthesized by similar procedures. $AlCl_3 \cdot 6H_2O$ (4.0 g) and 5-hydroisophthalic acid (3.0 g) were dissolved in H_2O (48 ml) and DMF (12 ml), respectively, under stirring. The mixture was placed in a 100 ml Teflon-lined steel autoclave and heated to 135 ℃, and held for 12 h in a convection oven. After being cooled to room temperature, the obtained solid was dispersed in EtOH and sonication in water at 70 ℃ for 3 h. The mixture was then filtered and washed with EtOH. This procedure was repeated two times. Finally, the obtained solid was dried for 100 ℃ for 2 h under an air condition.

3 Synthesis of CAU-10-F

$Al_2(SO_4)_3 \cdot 18H_2O$ (4.0 g) and 5-fluoroisophthalic acid (2.2 g) were dissolved in H_2O (27 ml) and DMF (7 ml), respectively. The mixture was placed in a 100 ml Teflon-lined steel autoclave and kept in an oven at 120 ℃ for 12 h. After the product was cooled to room temperature, the purification was carried out in the same manner as in the preparation of CAU-10-OH.

4 Synthesis of CAU-10-NO_2

$AlCl_3 \cdot 6H_2O$ (4.0 g) and 5-nitroisophthalic acid (3.5 g) were dissolved in H_2O (47 ml) and DMF (14 mL), respectively. The mixture was placed in a 100 ml Teflon-lined steel autoclave and kept in an oven at 120 ℃ for 12 h. After the product was cooled to room temperature, the purification was carried out in the same manner as in the preparation of CAU-10-OH.

5 Synthesis of CAU-10-NH_2

$Al(NO_3)_3 \cdot 9H_2O$ (4.0 g) and 5-aminoisophthalic acid (3.5 g) were dissolved in H_2O (47 ml) and DMF (14 mL), respectively. The mixture was placed in a 100 ml Teflon-lined steel autoclave and kept in an oven at 120 ℃ for 12 h. After the product was cooled to room temperature, the purification was carried out in the same manner as in the preparation of CAU-10-OH.

6 Synthesis of CAU-10-CH_3

$AlCl_3 \cdot 6H_2O$ (4.0 g) and 5-methylisophthalic acid (2.0 g) were dissolved in H_2O (25 ml) and DMF (7 ml), respectively. The mixture was placed in a 100 ml Teflon-lined steel autoclave and kept in an oven at 120 ℃ for 12 h. After the product was cooled to room temperature, the purification was carried out in the same manner as in the preparation of CAU-10-OH.

Table S11. Synthesis composition for CAU-10(Al)-X

	Metal precursor	Solvent (H_2O)	Ligand	Solvent (DMF)
CAU-10-H	$Al(NO_3) \cdot 9H_2O$ (4.0 g)	36 ml	Isophthalic acid (2.0 g)	10 ml
CAU-10-OH	$AlCl_3 \cdot 6H_2O$ (4.0 g)	48 ml	5-hydroxyisophthalic acid (3.0 g)	12 ml
CAU-10-F	$Al_2(SO_4)_3 \cdot 18H_2O$ (4.0 g)	27 ml	5-fluoroisophthalic acid (2.2 g)	7 ml
CAU-10-NO_2	$AlCl_3 \cdot 6H_2O$ (4.0 g)	47 ml	5-nitroisophthalic acid (3.5 g)	14 ml
CAU-10-NH_2	$Al(NO_3) \cdot 9H_2O$ (4.0 g)	25 ml	5-aminoisophthalic acid (2.0 g)	7 ml
CAU-10-CH_3	$AlCl_3 \cdot 6H_2O$ (4.0 g)	47 ml	5-methylisophthalic acid (3.0 g)	14 ml